

# Automatic Detection of Coil Position in the Chest X-ray Images for Assessing the Risks of Lead Extraction Procedures

YingLiang Ma<sup>1\*</sup>, Vishal S Mehta<sup>2</sup>, C. Aldo Rinaldi<sup>2</sup>, Pengpeng Hu<sup>3</sup>, Steven Niederer<sup>4</sup>,  
Reza Razavi<sup>4</sup>

<sup>1</sup> School of Computing Sciences, University of East Anglia, UK

<sup>2</sup> Department of Cardiology, Guy's & St. Thomas' Hospitals NHS Foundation Trust, London, UK

<sup>3</sup> Centre for Computational Science and Mathematical Modelling, Coventry University, UK

<sup>4</sup> School of Imaging Sciences and Biomedical Engineering, King's College London, UK

\* yingliang.ma@uea.ac.uk

**Abstract.** The lead extraction procedures are for the patients who already have pacemaker implanted and leads need to be replaced. The procedure is a high-risk procedure and it could lead to major complications or even procedure-related death. Recently, an Electra Registry Outcome Score (EROS) was designed to create a risk assessment tool using the data about personal health records and an accuracy of 0.70 was achieved. In this paper, we hypothesized that a coil inside the superior vena cava (SVC) is a very important risk factor. By integrating it into the risk assessment model, the accuracy can be further improved. Therefore, an automatic detection method was developed to localize the positions of coils in the X-ray images. It was based on a U-Net convolutional network. To determine the coil position relative to the SVC position inside the chest X-ray image, the heart region was first detected by using a modified VGG16 model. Then, the bounding box of the SVC can be estimated based on the heart anatomy. Finally, a XGBoost classifier was trained on the data about personal health records and the risk factor about the coil position. An accuracy of 0.85 was achieved.

**Keywords:** Deep learning, Wire detection, Risk assessment.

## 1 Introduction

The number of patients with implantable pacemaker has grown exponentially in recent decades. Transvenous lead extraction (TLE) is the primary treatment for complications related to the implanted pacemaker. The complications include lead fracture, device failure, lead erosion and infection [1]. Although the success rate of TLE procedure remain high, the procedure is sometimes complex and leads to severe complications and even procedure-related death. The studies in major European centers have reported a 1.7% rate of major complications including deaths [2]. Therefore, it is essential to assess the risk of the TLE procedure for individual patients to reduce the mortality rate. Sidhu et al [3] has proposed an Electra Registry Outcome Score (EROS) to create a risk

assessment tool using a number of variables about personal health data and an accuracy of 0.70 was achieved. Recently, machine learning (ML) based approaches have been proposed to improve the accuracy. Vishal et al [4] has trained ML models and tested them on a ELECTRa database [3] and achieved an accuracy of 0.74. The results are marginally improvement from EROS.

We hypothesized that adding additional information extracted from a plain chest X-ray image will further improve the accuracy. The coil inside the superior vena cava (SVC) is a very important risk factor as the common reason for the major complication inside the SVC is the fibrotic tissue around the lead or the coil. It does more likely happen to the coil which has a large surface area. The fibrotic tissue likely causes mechanical damages such as tear during the procedure [5]. To find out the coil position, the plain chest X-ray images were used and they are normally acquired before the procedure. Robust computer vision algorithms were designed, which are based on deep learning techniques for image segmentation. The computer vision algorithms were able to automatically compute the positions of the coils in the X-ray image and detect whether majority of the coil is inside the SVC or not. The main contribution of this manuscript is the methodology of the development of a deep learning framework using the combination of an additional feature from images and other clinical data to achieve higher accuracy to detect high-risk patients. The proposed approach is not limited to the TLE procedure using the chest X-ray image and it could apply to assess the risk of other cardiac interventional procedures using X-ray or CT images.

## 2 The detection of coils in X-ray images

In the chest X-ray images from patients undergoing the TLE procedure, there are often coils mixing with leads. The leads are thin metal wires. On the other hand, the coils have a large surface area of electrodes and they often conduct strong currents to depolarize the heart. They can be recognized on x-ray images as focal areas of wire thickening. In order to robustly detect the position of all coils inside the X-ray image, a two-step approach was proposed. Firstly, both leads and coils were segmented by using a U-Net convolutional network [6] and this acted as the coarse region segmentation. Then, the masked images created from the coarse region segmentation were feed to the second U-net model to extract the exact location of the coils.

### 2.1 The detection of both leads and coils

To segment both leads and coils from X-ray images, a U-Net convolutional network was trained and tested by using a database of 737 chest X-ray images from 737 patients.

**Creating manual segmentations of leads and coils.** The manual segmentation of leads and coils in X-ray images is very time-consuming. To speed up, a vessel enhancement filter [7] was used to extract all wire-like objects and the result image was automatically binarized by an adaptive binarization method: Otsu's method [8]. Then an experienced clinician manually removed the objects which are not leads or coils. In

addition, the pacemaker and nearby wire segments were also removed as they are not useful for finding the coils. Figure 1 presented the process of manual segmentation.

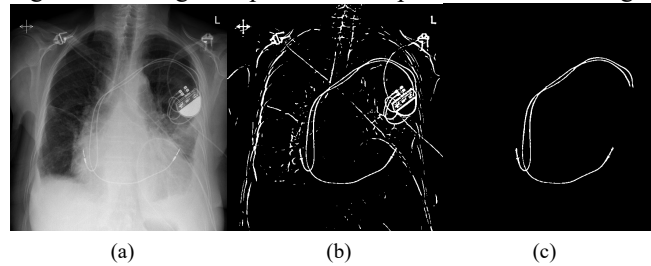


**Fig. 1.** Manual segmentation of leads. (a) The original image. (b) Image after applying the vessel enhancement filter. (c) The final result of manual segmentation.

The U-Net was trained to behave like a selective wire-enhancement filter and it is able to extract high-contrast leads and coils and ignore other wire-like objects such as surface ECG leads, rib bone shadows, the border of the cardiac silhouette and pacemaker.

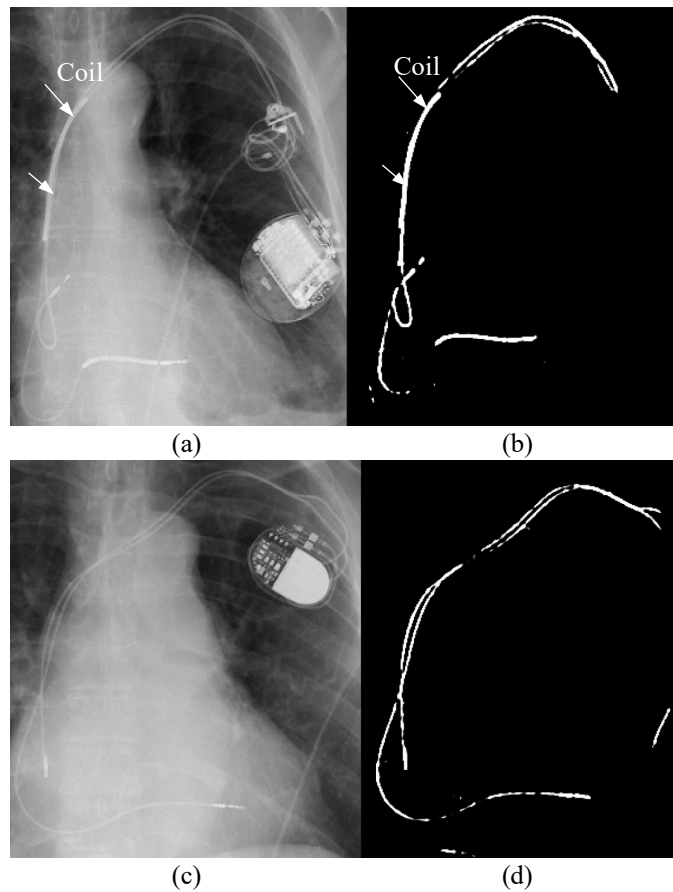


**Fig. 2.** The results of detecting leads and coils. (a)(c) The original image. (b)(d) The segmentation results output by the U-Net. (a) The coils are clearly within the detected segmentations.

**Training and results.** The ratio for train-test split is 70:30. The loss function for the U-Net model is the dice similarity coefficient (DSC) and it is defined as:

$$DSC = \frac{2|X \cap Y|}{|X| + |Y|} \quad (1)$$

The optimizer is Adam. The U-Net convolutional network was trained using 516 images. Images with the resolution of  $512 \times 512$  were directly input into the network without any down-sampling as the leads might not be visible in the low-resolution images. The U-Net model was implemented using TensorFlow API and training was carried out using an apple MacBook pro (GPU: Radeon Pro 560 and CPU: 2.9GHz quad-core Intel Core i7). The training process took about 8 hours and it was accelerated using GPU. The lengthy training process is because the high-resolution images ( $512 \times 512$ ) were used for training. The trained U-Net was tested on remaining 221 images. An accuracy of  $0.69 \pm 0.10$  was achieved for the segmentation of leads and coils and it was measured in DSC against the ground truth. Although the U-Net is not always able to detect the completed length of leads, it is sufficient for our next task: extracting coil position. The recall of coils is 1.0 and it means that all coils within X-ray images have been successfully detected as the coils are high-contrast objects and relatively easy to be detected. Two examples of segmentation results are presented in figure 2.

## 2.2 The detection of coils

To localize the exact location of the coils within the X-ray images, we use the results of detected leads and coils as the initial data input. Although the previous results already include the coils, the location of the coil relative to the location of SVC has to be determined as it is important to assess the risk of TLE procedures. [9] reported that the fibrotic tissue surrounding the coil is one of leading factors contributing to the mechanical damages such as tear during the procedure. To detect only the coil, the similar U-Net model is used but the input image is different. The input image is created by applying an image mask onto the original X-ray image and the mask is generated from the binary image after applying an image dilation operation with the kernel size of  $10 \times 10$ . The figure 3 illustrate the process of creating masked images.

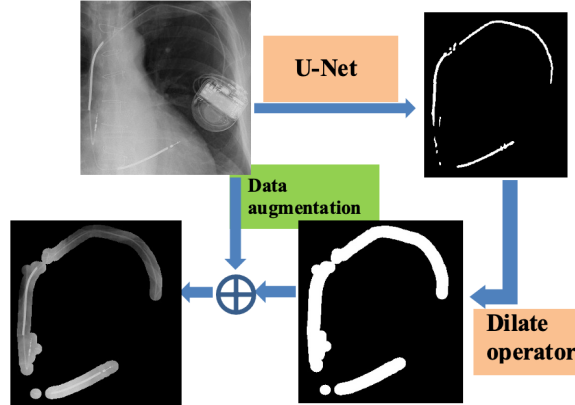


**Fig. 3.** The workflow of creating masked images for detecting the positions of coils.

In order to reduce the distraction from the thin lead wires, the input images were down-sampled to 256x256 and they are used as input data for the U-Net model. The U-Net is the same as the previous one except the dimension of input and output data. As the low-resolution images reduced the computation cost of model training, we were able to apply the data augmentation technique to increase the number of training images. The contrast of the 516 images were reduced by a random factor between 0.6 to 0.9 to create additional 1,032 training images. The reason for reducing contrast is to improve the performance of coil detection for low-contrast X-ray images. Therefore, the image masks were applied onto 1,548 training images and masked images were created. They are used as input images for the U-Net model. The training time is about 3 hours using the same PC which trained the previous U-Net model. As shown in figure 4, the accuracy of model training using data augmentation increases faster than the accuracy of model training without it.

Finally, the trained U-Net was tested on remaining 221 images. An accuracy of  $0.87 \pm 0.10$  was achieved for the detection of coils and it was measured in DSC against the ground truth. To measure the performance of U-Net with or without data augmentation, key metrics such as accuracy, precision, recall and F1-score were calculated and presented in table 1. A true positive detection is defined as at least 75% length of the target coil object was detected. A false positive detection is defined as the other wire object was detected as the target coil object. The examples of successful and unsuccessfully detections are presented in figure 5.

**Table 1.** Key metrics for model performance with or without data augmentation.

Data augmentation	Accuracy	Precision	Recall	F1 score
without	0.87	0.88	0.91	0.89
with	0.98	0.98	0.99	0.98

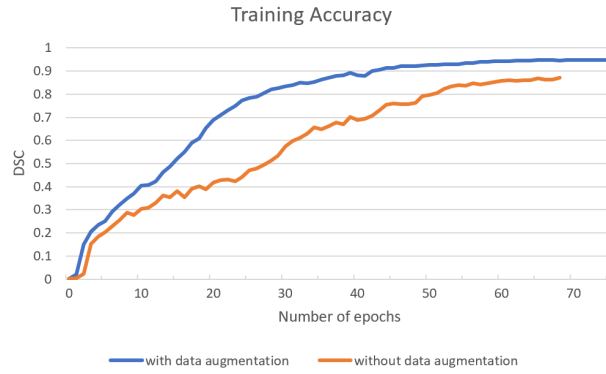


Fig. 4. Accuracy by epochs of the U-Net training in terms of the DSC.

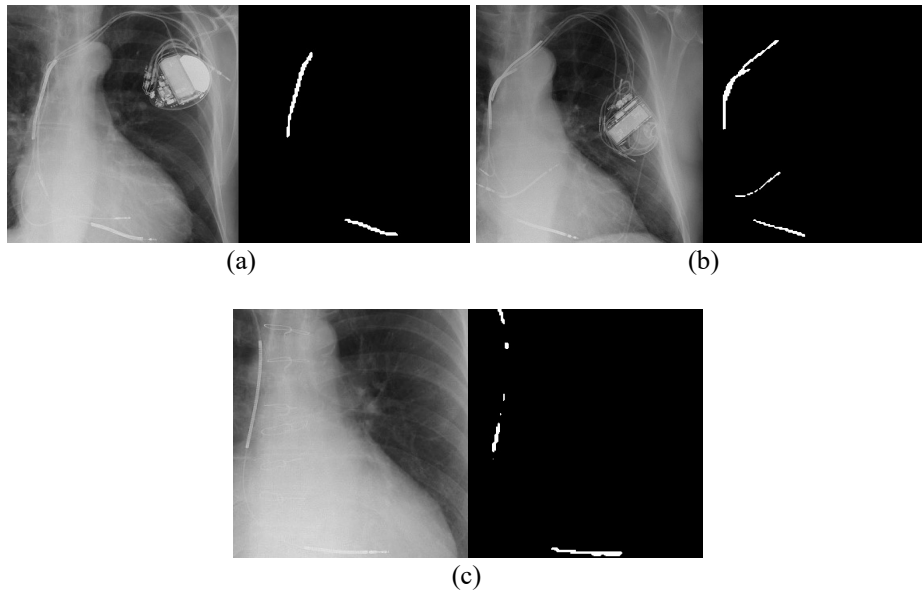


Fig. 4. Examples of coil detections. (a) (b) Successful detections. (c) A false negative detection which only part of coil (less than 75%) has been detected.

### 3 The detection of the approximate location of SVC

SVC is a major blood vessel inside the heart and it provides an important pathway for inserting the pacing leads into the right atrium and other heart chambers. The SVC is the most common location requiring surgical repair as the result of a major complication after the TLE procedure. It is not possible to detect the exact location of SVC in

the X-ray image as the SVC is not visible in the image unless a contrast agent is injected. However, it is possible to estimate the location based on the heart anatomy. As show in figure 5a, the location of the SVC (green box) is the top left corner of the heart region (red box). The height of the green box is approximately half the height of the heart region. The width of the green box is approximately one third of the heart region. The method was verified by overlaying 3D anatomy models (extracted from pre-procedure CT scan) with the chest X-ray image (figure 5b).

**The detection of the heart region.** To automatically located the SVC in the X-ray image, the heart region needs to be detected. A transfer learning approach was used to detect the heart region via bounding box regression, which is based on a modified VGG16 model. As shown in figure 6, the last 3 pre-trained fully-connected layers of a standard VGG16 model have been removed and replaced with 4 full-connected layers. The last layer outputs the coordinates of two corners positions of the bounding box. The modified VGG16 model uses the pre-trained weights [10] and it was re-trained using the manual annotations of the heart region in X-ray images.

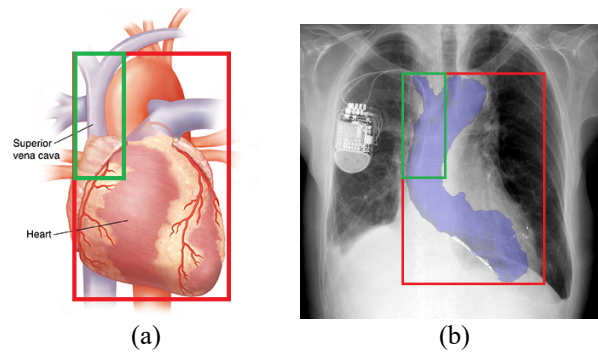


Fig. 5. (a) A medically accurate illustration of the anatomy of the heart. The red box is the region of the heart and the green box is the location of the SVC. (b) Overlaying 3D anatomy models with the X-ray image. The blue shadow is the 3D model of aorta, left ventricle and the SVC. The red box is the region of the heart and the green box is the location of the SVC.

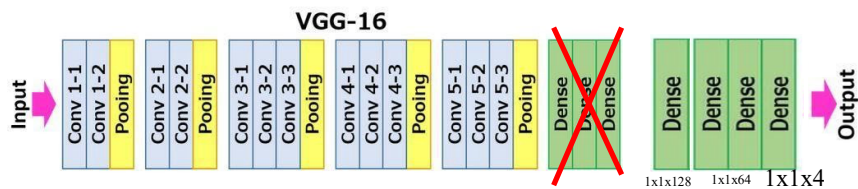


Fig. 6. The architecture of the modified VGG16 model.

**The accuracy of detection.** The accuracy of heart region detection is measured by the Intersection Over Union (IOU). IOU in this application is defined as:

$$IOU = \frac{|B_p \cap B_{gt}|}{|B_p \cup B_{gt}|} = \frac{|B_p \cap B_{gt}|}{|B_p| + |B_{gt}| - |B_p \cap B_{gt}|} \quad (2)$$

where  $B_p$  is the predicted bounding box or the detected bounding box and  $B_{gt}$  is the ground truth bounding box. A correct detection is that IOU is larger than or equal to the preset threshold. The preset threshold in this application is set to both 50% and 75%, as the detection of heart region has to be accurate to ensure that the location SVC is relatively accurate. An example of IOU was presented in figure 7. The precisions and recalls of the detect method were given in table 2.

**Table 2.** The precisions and recalls for assessing the accuracy of heart region detection.

IOU Threshold	50%	75%
Precision	1.0	0.818
Recall	1.0	1.0

(a)
(b)

Fig. 7. (a) The results of IOU. The green box is the ground truth and the red box is the detected bounding box. (b) The coil position related to the SVC. The green box is the bounding box of the SVC and the red box is the bounding box of the heart region. The yellow lines are the centerlines of the detected coils.

#### 4 Machine-learning model for risk assessment

Once the coil position was determined, it was compared with the bounding box of the SVC. If 50% of the coil length is within the SVC, the coil will be labelled as “inside”. Otherwise, the coil will be labelled as “outside”. The coil position label combined with personal health records were feed into a machine-learning model to predict the TLE procedure risk. The XGBoost classifier [11] was chosen to predict the risk of TLE procedures as it uses sequentially-built shallow decision trees to provide accurate results and a highly-scalable training method that avoids overfitting. Furthermore, the XGBoost classifier has been used to diagnose chronic kidney disease [12] and detect credit card fraud [13] because it works well with imbalanced datasets and binary classifications. There is a total 737 sets of data from 737 TLE clinical cases and the outcome from 18 cases (2.4%) are a major complication or procedure related death. To balance the data, Adaptive Synthetic (ADASYN) sampling techniques [14] were applied to the



data and generated additional 701 sets of data which was labelled as the cases of a major complication or procedure related death. The balanced data were split into two groups. 70% of data were used for training and 30% of data were used for testing. The learning rate was set to 0.02 and the number of gradient boosted trees was set to 200. The maximum depth of a tree, the minimum child weight and the subsample ratio of columns for each tree were set to 5, 1 and 0.75, respectively. The balanced accuracy of 0.85 was achieved, which was tested on the balanced test dataset.

## 5 Conclusions and future work

This paper presents a novel deep-learning framework for predicting the risk of the TLE procedures. Robust computer vision algorithms were developed to extract the position of coils in the chest X-ray images. By comparing the coil positions with the estimated location of the SVC, a new risk-factor variable was created. By adding this risk-factor variable with the personal health data, we were able to achieve a higher classification accuracy for detecting high-risk cases in the TLE procedures. Our approach only use plain chest X-ray images as the additional data source and the chest X-ray images are routinely acquired before the TLE procedures. Therefore, our approach does not require additional data and will not change current clinical practices for the TLE procedures.

Additional geometric features such as the number of overlapping leads inside the SVC, the angulation of a lead inside the right ventricle and the angulation of the lead near the entry point of the SVC could be important for further improvement of the risk modelling and achieve a higher classification accuracy.

## 6 Acknowledgement

This work is funded by a EPSRC grant (EP/X023826/1). The study was also supported by the Wellcome/EPSRC Centre for Medical Engineering (WT203148/Z/16/Z) and the National Institute for Health Research (NIHR) Biomedical Research Centre based at Guy's and St Thomas' NHS Foundation Trust and King's College London. The views expressed are those of the author(s) and not necessarily those of the NHS, the NIHR or the Department of Health.

## References

1. van Erven et al.: Attitude towards redundant leads and the practice of lead extractions: a European survey. *Europace* 12(2), 275–276 (2010).
2. Bongiorni, M. G., et al.: The European Lead Extraction ConTRolled (ELECTRa) study: A European Heart Rhythm Association (EHRA) Registry of Transvenous Lead Extraction Outcomes. *European Heart Journal* 38(40), 2995–3005 (2017).
3. Sidhu, B. S., et al: Risk stratification of patients undergoing transvenous lead extraction with the ELECTRa Registry Outcome Score (EROS): an ESC EHRA EORP European lead extraction ConTRolled ELECTRa registry analysis. *Europace* 23(9), 1462–1471 (2021).

4. Mehta, V. S., et al.: Machine learning–derived major adverse event prediction of patients undergoing transvenous lead extraction: Using the ESC EHRA EORP European lead extraction ConTRolled ELECTRa registry. *Heart Rhythm* 19(6), 885-893 (2022).
5. Tułeckki, Ł., et al.: A Study of Major and Minor Complications of 1500 Transvenous Lead Extraction Procedures Performed with Optimal Safety at Two High-Volume Referral Centers. *International journal of environmental research and public health* 18(19), 10416-29 (2021).
6. Ronneberger, O., et al.: U-Net: Convolutional Networks for Biomedical Image Segmentation. In: *Proc. Int. Conf. Medical Image Computer Assisted Intervention (MICCAI), LNCS, vol 9351*, pp. 234–241. Springer (2015).
7. Frangi, A. F., et al.: Multiscale vessel enhancement filtering. *Proc. Int. Conf. Medical Image Computer Assisted Intervention (MICCAI)* (1998).
8. Otsu, N.: A threshold selection method from gray-level histograms. *IEEE Transactions on Systems, Man and Cybernetics* 9(1), 62–66 (1979).
9. Tułeckki, Ł., et al.: Analysis of Risk Factors for Major Complications of 1500 Transvenous Lead Extraction Procedures with Especial Attention to Tricuspid Valve Damage. *International journal of environmental research and public health* 18(17), 9100-9113 (2021).
10. J. Li, et al.: Transfer Learning Performance Analysis for VGG16 in Hurricane Damage Building Classification. *2nd International Conference on Big Data & Artificial Intelligence & Software Engineering (ICBASE)*, pp 177-184. (2021).
11. Chen, T., et al.: XGBoost: A Scalable Tree Boosting System. *Proceedings of the 22nd ACM SIGKDD International Conference on Knowledge Discovery and Data Mining (KDD '16)*, pp 785–794. (2016).
12. Ogunleye, A., et al.: XGBoost Model for Chronic Kidney Disease Diagnosis. *IEEE/ACM Transactions on Computational Biology and Bioinformatics* 17(6), 2131-2140 (2020).
13. Abdulghani, A. Q., et al: Credit Card Fraud Detection Using XGBoost Algorithm. *14th International Conference on Developments in eSystems Engineering*, pp. 487-492 (2021).